Supporting Information for the manuscript

Large thermoelectric power factor enhancement observed in InAs nanowires

By Phillip M Wu, Johannes Gooth, Xanthippi Zianni, Sofia Fahlvik Svensson, Jan Göran Gluschke, Kimberly A Dick, Claes Thelander, Kornelius Nielsch, Heiner Linke

Comparison of measured thermovoltages to earlier measurements

For large V_G, where the carrier concentration $n \approx 10^{17}$ cm^{-2}, we find $S \approx$ -10 μV/K at T = 100 K for our wires, comparable to S(100K) = -20 μV/K reported for bulk InAs with n~10^{18} cm^{-3} [1]. The value measured here can also be compared to earlier measurements reported for InAs nanowires, for example S(100 K) = -20 μV/K for a D = 155 nm wire [2], S(100 K) = -120 μV/K for a 65 nm wire [3], and S(100 K) ≈ - 6 μV/K for a D = 20 nm wire [4]. These values varied considerably, which may in part be attributed to variations in the Fermi energy between these wires.

Estimation of carrier concentration and mobility

The carrier mobility of the nanowires has been estimated from the conductance measurements $G(V_G)$ and by using [5]

$$\mu = \frac{dI_{bias}}{dV_G} \cdot \frac{L^2}{V_{bias} C},$$

where dI/dV_G is the transconductance, L the active nanowire channel length and C the capacitance. The capacitance between the nanowire and the backgate contact was numerically calculated using a two dimensional electrostatic model in COMSOL Multiphysics. The carrier concentration is then calculated from

$$n = \frac{I_{bias} L}{q \mu V_{bias} A}$$

where $A = \pi(D/2)^2$ is the cross section of the nanowire and q the elementary charge [5].

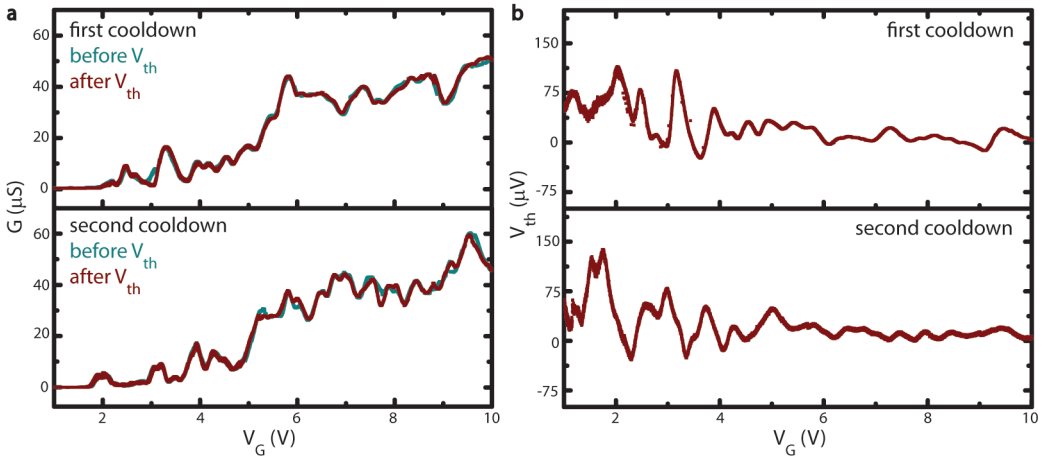

Figure S1. **Reproducible fluctuations in G and V_{th}**. The fluctuations observed in G and V_{th} as a function of back gate voltage V_G (see for example Fig. 2) are highly reproducible within one cooldown, but change upon thermal cycling. This indicates that surface charges, which are known to reconfigure upon thermal cycling and which can induce an electrostatic modulation of the nanowire width, are one origin of the fluctuations G and V_{th}. **a**, The conductance G of NW4 (D = 69 nm, L = 0.77 μm) as a function of V_G. The features in the conductance are reproducible within one cooldown and do not shift after a thermal gradient has been applied, but they are not reproduced when the sample is thermally cycled. The conductance was measured with a source-drain bias V_{sd} = 2 mV. **b**, The features in thermovoltage V_{th} also change considerably from cooldown to cooldown and are correlated to the corresponding conductance traces in **a**. The thermovoltages were taken at a heating power of P_H = 0.38 mW. All data shown in this figure were taken at a base temperature of 1.6 K.

In conclusion, these data show that the observed fluctuations in G, V_{th} and thus $S^2\sigma$ (which is calculated from the measured G and V_{th}) are *not* noise, but highly reproducible features that can be attributed to interference effects. However, the fact that the fluctuations change upon thermal cycling indicates that the *details* of the fluctuations are

determined by subtle details of the potential felt by the electrons in the wire, including surface charges that can reconfigure upon warming to room temperature. These details are currently outside experimental control, and can thus also not be modeled precisely or quantitatively.

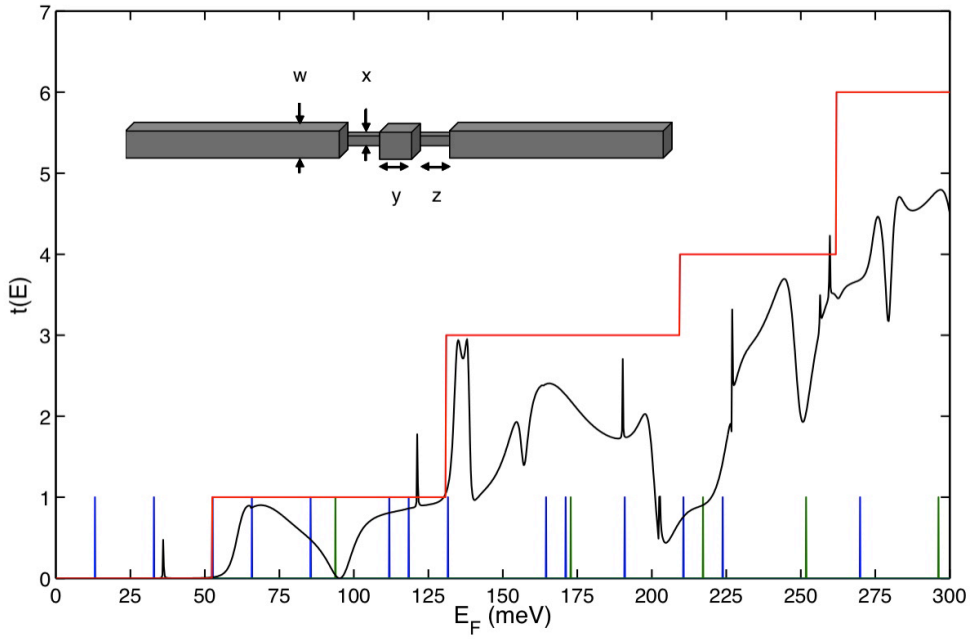

Figure S2 Theoretical simulations. Fluctuations in the transmission function $t(E)$ (which is closely related to the conductance G at low temperatures) of a nanowire occur when 0D resonances (formed because of quantum-dot-like states occurring in small, geometrically constricted wire segments) interfere with the nanowire 1D propagating waves. The dot-like states are here shown as blue and green lines. Whereas the occurrence of such states is a generic feature of non-uniformities in nanowires, their details (exact position and magnitude) of the states (and thus of the fluctuations in G) depends on the details of the non-uniformity used by the model. The black line shows $t(E)$ of a non-uniform nanowire modulated as shown in the schematic for w = 50 nm, x = 25 nm, y = 20 nm, z = 20 nm. The vertical lines show the resonant states of InAs dots of dimensions 25 x 25 x 20 nm (green) and 50 x 50 x 20 nm (blue). The transmission coefficient of a uniform nanowire of diameter 25 nm (red) is also shown. The fluctuations in $t(E)$ are clearly correlated with the 0D resonances.

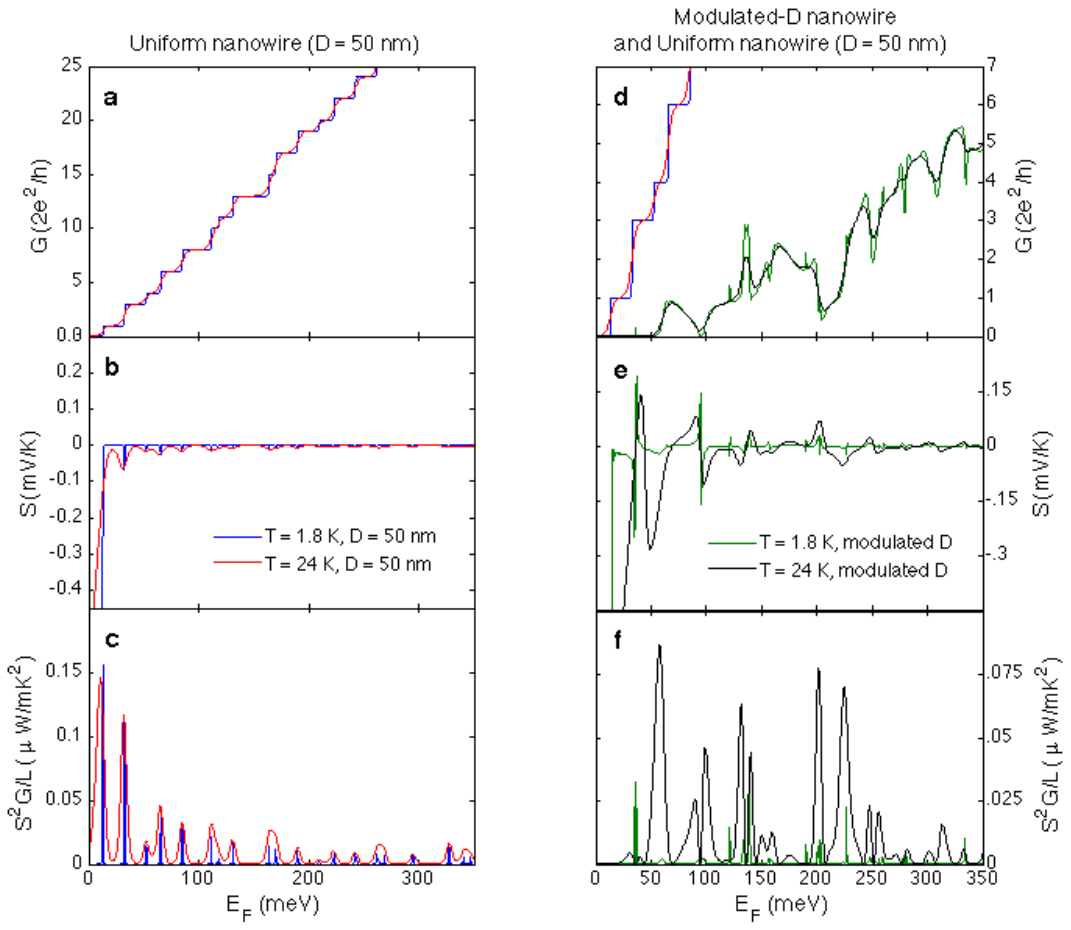

Figure S3 Comparison of simulation results for uniform and modulated-diameter nanowires. Comparison of the thermoelectric properties at T = 1.8 K and 24 K of a uniform, ballistic nanowire (D = 50 nm) **(a-d)** and a modulated nanowire **(d-f)** with dimensions w = 50 nm, x = 25 nm, y = 20 nm, z = 20 nm, as defined in the inset to Figs. 2 and S4). We point out the following features: **d,** compared to the uniform nanowire, the conductance threshold of the non-uniform wire is shifted to higher E_F. As a consequence, in the non-uniform wire, the conductance is suppressed at the E_F where the S reaches large values **d, e**. Therefore, whereas the uniform wire exhibits a peak power factor just below the first subband **c**, the non-uniform wire doesn't exhibit this peak, **f.** Instead, the non-uniform wire exhibits a dense series of power factor peaks, observed in this work,

over a wide range of E_F related to the 0D resonances (see Fig. S2). Note that the highest power factor peak, below the first subband in **c,** is very narrow (full width half maximum ~ 0.6 meV at 1.8 K), and has never been observed in experiments. **e**, the *S* of the non-uniform wire exhibits characteristic oscillation between positive and negative values that are typical for 0D resonances, and that are not observed in uniform 1D wires, **b.**

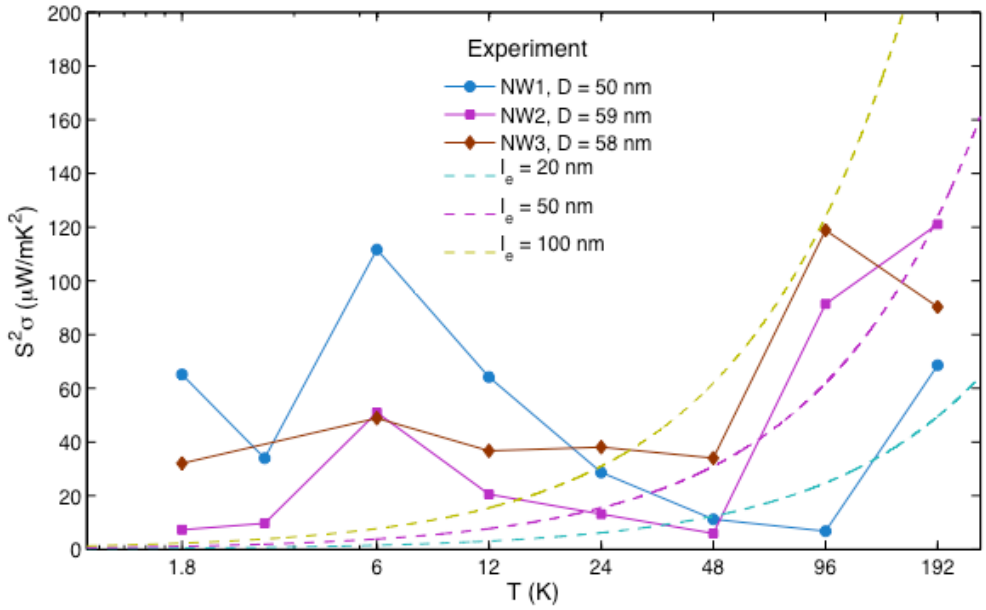

Figure S4. Enhanced average thermoelectric power factor in InAs nanowires. Carrier-concentration averaged values of $S^2\sigma$ for NW1, NW2, and NW3, obtained as the mean over the gate voltage range [6 V, 10 V] (see Fig. 2a-d), which provides an estimate of the expected $S^2\sigma$ for an ensemble of wires with similar diameter, but with wire-to-wire variations in the precise wire shape and carrier concentration. The average is done in the following way: at each fixed substrate temperature, we find the average power factor in the gate voltage range from 6 V to 10 V. Although not as high as the peak values, an enhancement in power factor is observed, demonstrating that the enhancement is not sensitive to exact positioning of E_F. We estimate (see below) that the gate voltage range used corresponds to a variation of E_F by 6 - 10 meV, corresponding to 10 - 20 kT at 6 K. In comparison, the expected power factor peaks in a uniform wire (Fig. S3c) are only about 1 - 2 meV wide. This indicates that the power-factor enhancement effect discovered here is, in comparison to 1D confinement effects, much more stable against

variations in E_F and wire geometry. This tolerance greatly increases the potential to use this effect in future nanowire devices, such as nanowire arrays.

Estimate of Fermi energy variation in Fig. S4.

Two approaches were used to estimate the range of E_F that corresponds to the gate voltage range [6 V, 10 V] over which power-factor values were averaged in Fig. S4. First, E_F was estimated from measured S as a function of V_G, using the Boltzmann transport equation for a single type of charge carriers [6-8] (electrons) with effective mass 0.026 m_e and a 3D density of states. Lattice and boundary scattering were assumed to be dominant. For NW2 this model yields a rate of change in dE_F/dV_G from 13 meV/V near depletion to 2 meV/V in the range where the nanowire is highly conductive ($V_G \approx 10 – 12$ V) for temperatures below 50 K. Second, we estimated the lever arm of the Coulomb diamond for NW4 (Fig. 4) in the range V_G = 1.6 V to 3.6 V at 1.6 K and V_G = 2.0 V to 4.5 V at 1.6 K and 4 K to be 9.4 meV/V. Results from both models suggest that the E_F variation in the interval V_G = [6 V, 10 V] is about 6 - 10 meV.

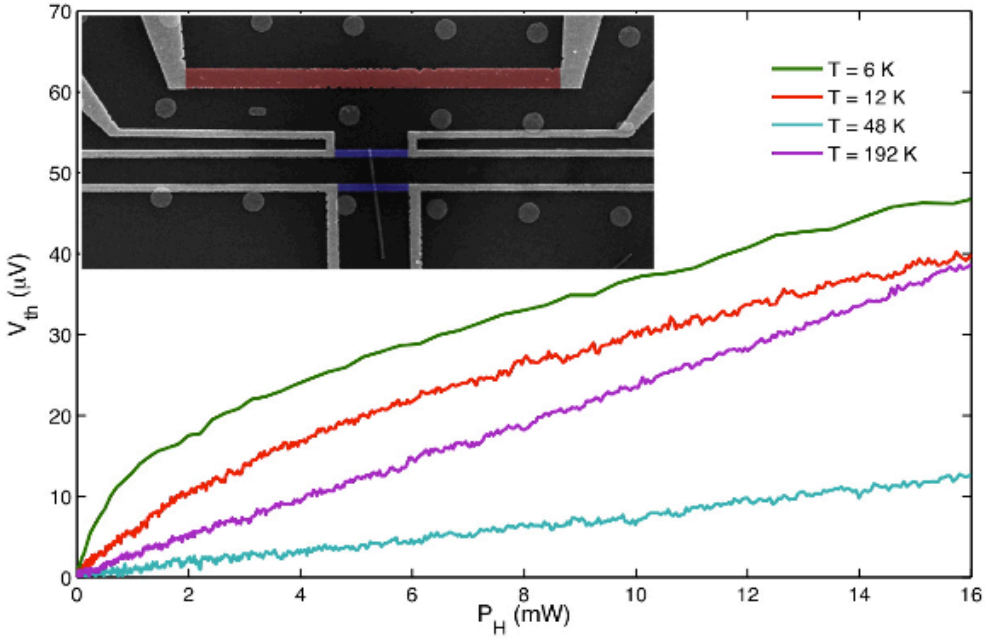

Figure S5. **Thermovoltage versus heating power**. Thermovoltage as a function of heating power for NW1 when the wire is conducting (V_G = 10 V). We calibrated the thermometers against the substrate temperature, which was defined by the base temperature of the sample stage in a variable temperature Janis cryostat. From this calibration, the temperature rise due to given, applied heating power P_H can be determined for the hot and cold sides separately. The P_H used (P_H = 0.3 - 1.6 mW) was chosen to ensure linear behavior of V_{th}. To estimate $P_H = I_H^2 R_H$, the resistance R_H of the heating strip, marked in red, was calculated using the resistivity of the metal layer, which was determined in a four point measurement of the thermometer strips, marked in blue. The applied current through the heating strip I_H was measured as a function of temperature. Note that we observe stronger nonlinear behavior of V_{th} with increasing P_H at lower V_G and at low T. This observation is in line with recently published data on

nonlinear thermovoltage in quantum dots [9], reinforcing our interpretation of the role of quantum-dot like states.

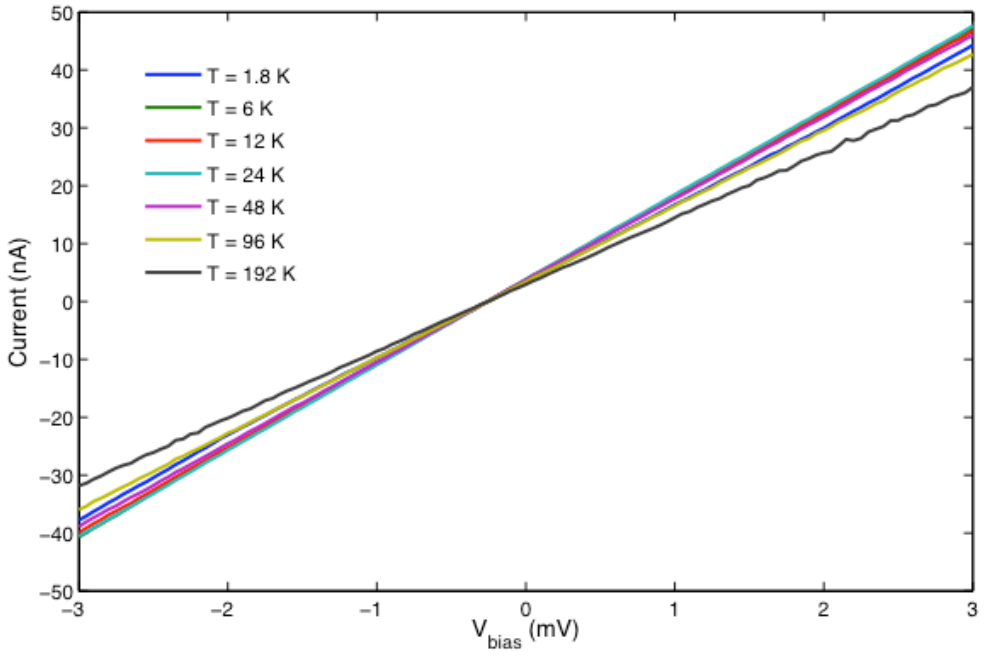

Figure S6. **Ohmic contact electrodes**. Current-voltage bias traces for NW1 (D = 50 nm) at V_G = 10 V. The good linearity indicates that the contacts are ohmic, and similar behavior is seen for all NWs studied in this work. A small offset at zero bias arises from the pre-amplifier. We take this into account when determining where the conductance reaches zero.

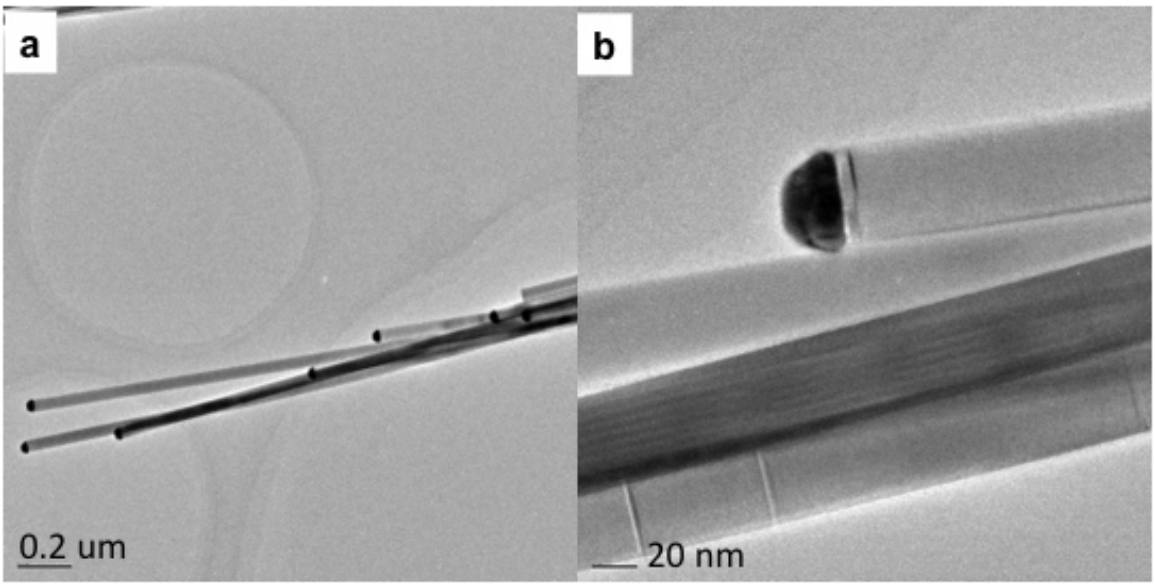

Figure S7. Transmission Electron Micrograph of InAs nanowires from the same batch. **a**, Nanowires lifted from the same growth substrate as NW1 onto a TEM grid for imaging. For each growth substrate, we deposited aerosol particles with one fixed diameter, and grew nanowires. As the image shows, nanowires from the same batch are similar in size. **b**, Zoomed in image of **a**. Note that the nanowires exhibit uniform diameter throughout the length of the nanowire, with little to no tapering.

References

1 Rode, D. L. Electron Transport in InSb, InAs, and InP. *Phys. Rev. B* **3**, 3287 (1971).

2 Mavrokefalos, A., Pettes, M. T., Saha, S., Zhou, F. & Shi, L. Combined Thermoelectric and Structure Characterizations of Patterned Nanowires. *IEEE International Conference on Thermoelectrics*, 234 (2006).

3 Zhou, F. *et al.* Thermal conductivity of indium arsenide nanowires with wurtzite and zinc blende phases. *Phys. Rev. B* **83**, 205416 (2011).

4 Tian, Y. *et al.* One-dimensional quantum confinement modulated thermoelectric properties in InAs nanowires. *Nano Letters* **12**, 6492-6497 (2012).

5 Dayeh, S. A. *et al.* High Electron Mobility InAs Nanowire Field-Effect Transistors. *Small* **3**, 326-332 (2007).

6 Lin, Y.-M., Sun, X. & Dresselhaus, M. S. Theoretical investigation of thermoelectric transport properties of cylindrical Bi nanowires. *Phys. Rev. B* **62**, 4610 (2000).

7 Nolas, G. S., Sharp, J. & Goldsmid, H. J. *Thermoelectrics*. (Springer, New York, 2001).
8 Seol, J. H. *et al.* Measurement and analysis of thermopower and electrical conductivity of an indium antimonide nanowire from a vapor-liquid-solid method. *Journal of Applied Physics* **101**, 023706 (2007).
9 Svensson, S. F. *et al.* Nonlinear thermovoltage and thermocurrent in quantum dots. *Arxiv: 1307.0617* (2013).